CENTRIFUGAL SPRAYING SYSTEM DESIGN AND DROPLET DISTRIBUTION CHARACTERIZATION FOR MAIZE PLANT PROTECTION UAV
/
玉米植保无人机离心喷施系统设计与雾滴分布特性试验

Jiaxun HE[1], Keke SUN[1], Taojie WANG[1], Zhihua SONG[1], Lichao LIU[1,2]
[1] College of Engineering, Anhui Agricultural University, Hefei, Anhui, 230036, China
[2] Engineering Laboratory of Intelligent Agricultural Machinery Equipment, Anhui, Hefei, 230036, China
Tel: +86 15705603452; E-mail: llchao@ahau.edu.cn
Corresponding author: Lichao Liu
DOI: https://doi.org/10.35633/inmateh-73-06

Keywords: *aviation spraying operation, centrifugal nozzle parameters, spraying system, droplet distribution characterization*

ABSTRACT
Aiming at the problem that the ground plant protection machine is difficult to enter for plant protection in the middle and late stages of maize field, this paper designs a UAV centrifugal spraying system for maize plant protection based on centrifugal nozzle and plant protection UAV. A single nozzle parameter test was carried out, and the results showed that the droplet size is related to the liquid supply flow rate and the nozzle speed. According to the optimal biological particle size theory, the nozzle parameters with the liquid supply flow rate of 1000 mL/min and the rotation speed of 14000 r/min are selected to test the droplet distribution characteristics under actual operation conditions, and the droplet size, droplet density, coverage and other important indicators of aviation spraying operations are analyzed. The experimental results show that the flight speed of the UAV significantly affects the droplet distribution in the bottom layer of maize. The droplet coverage and droplet deposition of each sampling layer decrease with the increase of flight speed. When the flight speed is 1.5 m/s, the coefficient of variation of the centrifugal spraying system is the smallest, and the droplet deposition effect is the most uniform. This study can provide a reference for the parameter optimization and correct use of centrifugal plant protection UAV in the middle and late plant protection operations of high-stalk crops such as maize.

摘 要
针对玉米中后期田间郁闭，地面植保机难以下田进行植保的问题，本文基于离心喷头和植保无人机设计了一款用于玉米植保的无人机离心喷施系统。开展了单喷头参数试验，结果表明：雾滴粒径与供液流量、喷头转速均相关，且结合最佳生物粒径理论，选择供液流量为 1000 mL/min，转速为 14000 r/min 的喷头参数进行实际作业情况下的雾滴分布特性试验，分析雾滴粒径、雾滴密度、覆盖率等航空喷施作业的重要指标。试验结果表明：无人机的飞行速度显著影响玉米底层的雾滴分布，各采样层的雾滴覆盖率和雾滴沉积量的变化趋势均随着飞行速度的增大而减小，在飞行速度为 1.5m/s 时离心喷施系统的变异系数最小，雾滴沉积效果最均匀。该研究为离心喷头植保无人机在玉米等高秆作物中后期植保作业的参数优化和正确使用提供参考依据。

INTRODUCTION
Maize is one of the three major food crops in China, widely planted and with high yield, not only an important food resource, but also an important raw material in industry and animal husbandry, with high market and social value. The Huang-Huai-Hai region is the main planting area of summer maize in China, since 2015, the Ministry of Agriculture and Rural Development has organized the zero-growth action of chemical fertilizer and pesticide use, and after several years of implementation, the utilization rate of pesticides in China has significantly improved. However, in the middle and late stage of maize growth, the plants are high and the closed rows are formed by field depression. The efficiency of traditional artificial application is low, while the existing spray rod sprayer is difficult to enter, and the injury rate is high (*Liu et al., 2022*), and most of the sprayer use pressure nozzle, easy to block. Vigorously promoting green control and precision scientific medication, the use of plant protection drones for maize mid- and late-stage pest control is currently a more reasonable solution (*Xie et al., 2022; Yang et al., 2020*).

China's plant protection UAVs use atomization nozzle is mainly divided into pressure nozzle and centrifugal nozzle, pressure nozzle in the requirement of small droplet size is easy to block, centrifugal nozzle particle size change can be controlled by the rotational speed in real time (*Chen et al., 2018*). Compared to pressure nozzles, centrifugal nozzles have better atomization, pesticide cost savings, and long life span in spraying facilities (*Dong et al., 2018*). *Yu et al., (2023)*, developed a rotary nozzle for UAV spraying, and explored the influence of three factors on the droplet size of the centrifugal nozzle from the flow rate, rotation speed and mesh number, which provided a certain technical basis for the research and optimization of the spray parameters of the centrifugal nozzle. *Chen et al., (2023)*, used CFD simulation to study the downwash airflow and droplet distribution of the six-rotor UAV, and combined RBFNN and GA to optimize the parameters of the spraying system. *Jane et al., (2021*), conducted experiments in vineyards, and three different types of drones and two different types of nozzles were evaluated. It was concluded that the vortex airflow and the arrangement position of the nozzle were the two main reasons affecting the difference in spray performance. *Gavali et al., (2023)*, used PIV technology to study the droplet deposition characteristics of centrifugal sprayers, and concluded that at a constant rotational speed, the friction force between the ejected liquids decreases, and changing the liquid mass will cause the droplet diameter to increase. *Chen et al., (2017)*, studied the effect of wind field on the penetration and uniformity of droplet deposition in the effective spraying area through the actual spraying operation test. *Fritz et al., (2009)*, investigated the effect of different flight speeds of plant protection aircraft on the particle size of fog droplets using wind tunnel testing methods. *Biglia et al.,* (*2022*), carried out experiments on fog droplet deposition in vineyards with different flight speeds of drones and spray nozzles, and the results showed that: the flight speed of the drones had a significant effect on the amount of fog droplet deposition in different canopies of grapes. All the above studies provide reference for the optimization of nozzle operation parameters, but the spraying problem of high stalk dense planting crops has not been solved.

This paper designs a centrifugal spraying system applicable to plant protection drones, controls the rotational speed of the centrifugal nozzle through the wireless control module, and then changes the size of the droplet size, carries out a test on the droplet deposition and distribution characteristics of plant protection drones in the middle and late stages of maize, and investigates the parameter indexes such as the droplet size, density, coverage, and deposition rate of the maize field with different sample points, in order to provide references for the effective application of plant protection drones in maize in the middle and late stages of plant protection.

MATERIAL AND METHODS

DESIGN OF CENTRIFUGAL SPRAYING SYSTEMS FOR UAV

The structure of the maize plant protection drone is shown in Fig. 1, in which the drone platform adopts the DJI T20 plant protection drone, and the centrifugal spraying system consists of the centrifugal nozzle and wireless control system which are modularized and designed to form an independent system installed on the plant protection drone.

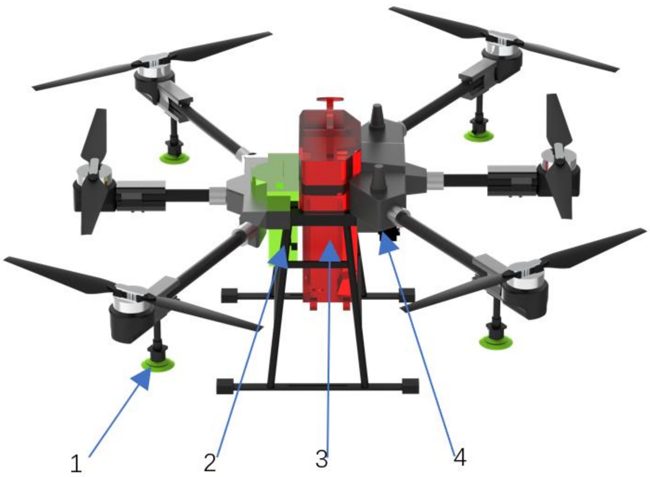

Fig. 1 - Schematic diagram of centrifugal plant protection drone structure

1. centrifugal nozzle; 2. plant protection drone; 3. medicine cabinet; 4. control box

The main structure includes centrifugal nozzle, liquid pipeline, microcontroller and remote control. When working, the remote control of the UAV controls the flow of the nozzle, and the start-stop and speed of the centrifugal nozzle are realized by the independently developed remote control system, which sends commands to the control box of the centrifugal spraying system through the hand-held remote control to realize the one-key start and speed regulation of the nozzle. The speed control process is realized by the microcontroller in the control box through PWM (pulse width modulation) technology, adjusting the duty cycle of PWM to control the rotational speed of the centrifugal spray nozzle to change the droplet size. The total weight of the centrifugal spraying system is small, which has less influence on the drug carrying capacity of the plant protection UAV, the weight of the centrifugal spraying system is 1 kg.

Nozzle structure

The plant protection UAV uses centrifugal nozzle, the main structure of the designed centrifugal nozzle is shown in Fig. 2a including the drive motor, atomizing disk, electronic speed controller and waterproof shell. The drive motor of the centrifugal nozzle adopts a brushless DC motor with 12 V power supply. The output shaft of the drive motor is connected to the end of the atomizing disk, and the atomizing disk is disc-shaped and divided into two parts, as shown in Fig. 2b and 2c. Controlled by the single-chip microcomputer, the brushless motors rotate to drive the atomizing disk. The liquid is sent to the atomization disk through the inlet. Under the action of centrifugal force, the liquid is shunted along the water tank on the atomization disc, and then atomized into small droplets through the fine line atomization groove. Finally, the small droplets are spiraled out through the atomizing groove on the outer edge of the tooth tip.

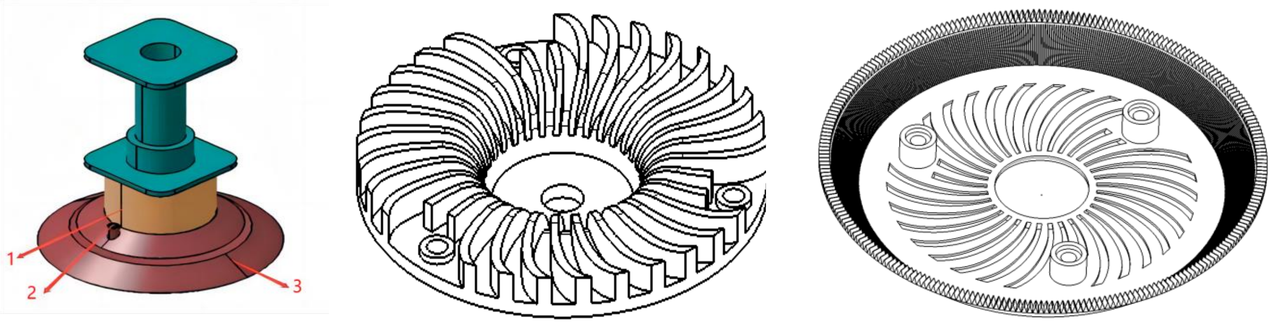

a) b) c)

Fig. 2 - Structure of nozzle and atomization disk

1. brushless motor; 2. Inlet; 3. fogging tray

Wireless control system for centrifugal nozzles

The wireless control system is designed to achieve the purpose of changing the droplet size by changing the rotational speed of the centrifugal nozzle, and the control system includes three modules: power supply module, nozzle control module, and remote control module.

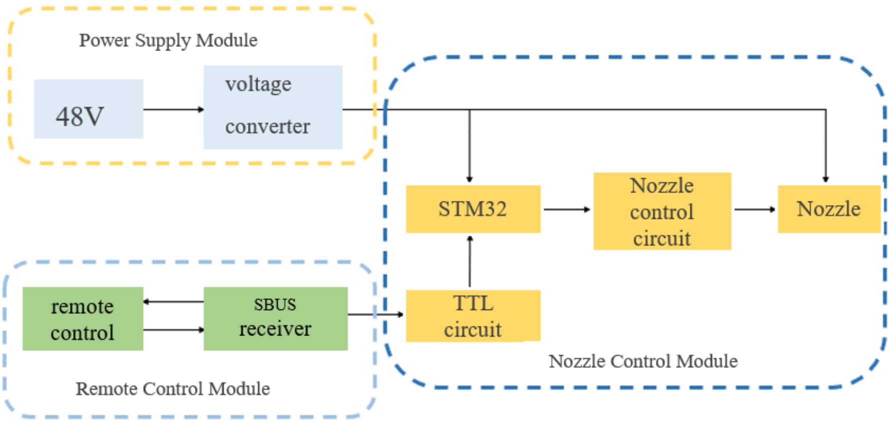

Fig. 3 - Control system composition

Power modules

As shown in Fig. 4, the whole control system is powered by the 51.8 V battery of the UAV, which is converted to 12 V and 3.3 V through the voltage conversion module. As shown in Fig. 5, the voltage is converted to 3.3 V by LDO voltage regulator PW8600 and linear circuit to provide power for the MCU main control chip and the remote control receiver, and converted to 12 V by DC-DC power supply chip PW2906 and buck circuit to provide power for the brushless ESC.

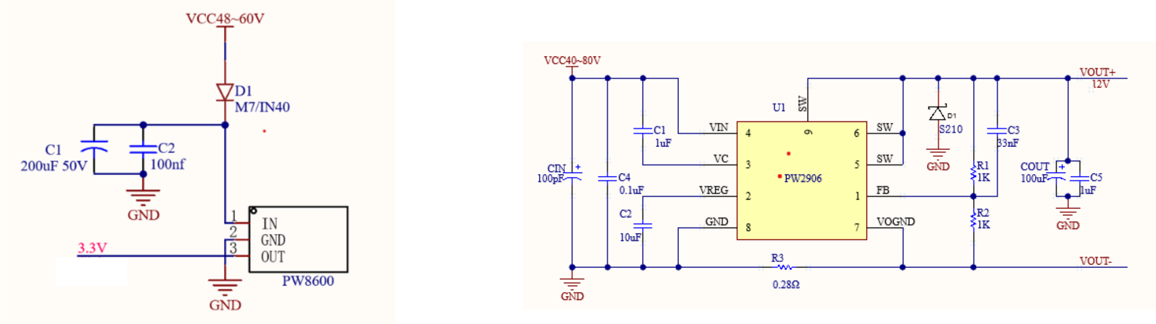

Fig. 4 - Circuit diagram of the power supply module of the control system

Remote control module

The remote control module is mainly a remote control, SBUS receiver. Through the handheld remote control commands are sent to the spraying system of the wireless receiver module in the control box. The remote control and receiver are selected from WFLY's ET08 and RD201W models, respectively. The remote control transmits key values to the receiver through a 2.4GHz wireless signal. The receiver communicates with the microcontroller through the SBUS serial port, and the microcontroller receives and parses the SBUS signal through the serial interrupt function in the program, converting the key value into a PWM wave value and transmitting it to the brushless electric controller to control the start stop, speed, etc. of the centrifugal nozzle.

Printhead control module

The start-stop and speed change of centrifugal nozzle is realized by the remote control system developed independently, and the microcontroller in the control box realizes the start-stop and speed change of centrifugal nozzle through PWM technology, and adjusts the duty cycle of PWM to control the rotational speed of centrifugal nozzle to change the size of droplet particle size. stm32 microcontroller accepts and analyzes the SBUS signal from the remote control module through the serial interrupt function of the program and converts the key value into PWM wave value, and amplifies the output signal through field effect tube to control the start-stop and rotational speed of centrifugal nozzle. The key value will be converted to PWM wave value, and through the field effect tube will be the output signal amplification, so as to control the centrifugal nozzle start-stop, speed and so on. Single nozzle control circuit diagram shown in Fig. 5.

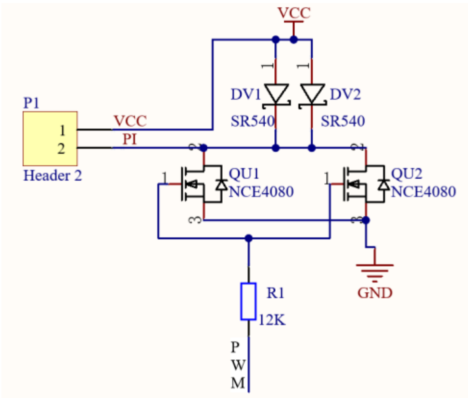

Fig. 5 - PWM control circuit

SINGLE NOZZLE PARAMETER TEST

Centrifugal nozzle speed and PWM signal duty cycle calibration

The atomization effect of the centrifugal nozzle is closely related to the rotational speed of the nozzle, the rotational speed of the centrifugal nozzle is controlled by adjusting the PWM duty cycle; in order to more accurately control the rotational speed of the nozzle, it is necessary to establish a deterministic function relationship between the PWM duty cycle and the motor speed. For this purpose, a laser speed meter is used to measure the centrifugal nozzle speed under different PWM, and the results are shown in Fig. 6.

As can be seen in Fig. 6, when the voltage is 12 V and the PWM frequency is 500 Hz, the centrifugal nozzle speed and the PWM duty cycle are approximately linear, and the centrifugal nozzle speed can be better controlled by adjusting the PWM duty cycle using the PWM signal generator.

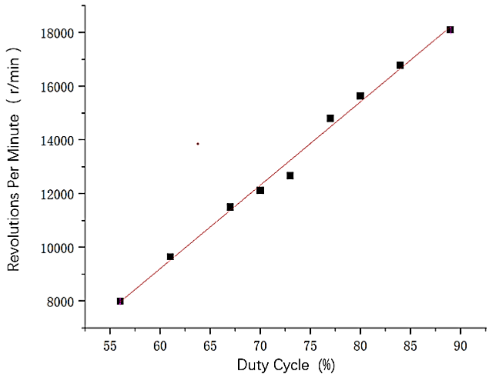

Fig. 6 - Relationship between nozzle speed and PWM duty cycle

Centrifugal nozzle speed and droplet size calibration

In order to clarify the numerical relationship between atomizing disk flow and motor speed and droplet particle size, and to find the centrifugal spray nozzle operating parameters with the bio-optimal particle size to satisfy plant diseases, the relevant tests were carried out in a suitable environment.

Test platform

A set of centrifugal nozzle parameter testing platform is designed, which mainly consists of centrifugal nozzle, brushless water pump, medicine tank, microcontroller, support frame and YE180-A laser particle size meter. The centrifugal nozzle is controlled by a wireless control system designed to change the speed of the centrifugal nozzle. The centrifugal nozzle, brushless water pump, and medicine tank are connected through transparent rubber hoses. The microcontroller controls the brushless water pump to change the flow rate of the nozzle, and the support frame can adjust the height of the nozzle according to testing needs. In the actual plant protection operations, the flight height of the UAV is usually higher than the crop canopy 1~3 m (*Qiu et al., 2013*), the test set the centrifugal nozzle from the laser particle size meter test beam 1.5 m, the transmitting end and the receiving end of the laser line is placed directly below the centrifugal nozzle, the laser particle size meter is connected to the computer, the computer running the laser particle size analyzer dedicated NKT analysis software can be derived from the Dv10, Dv50, Dv90 particle size distribution map and cumulative distribution map and other data. According to the purpose of this paper, Dv50 data is mainly used as the average particle size of droplet group to study the relationship between nozzle speed, flow rate and droplet particle size.

Taking into account the outdoor wind speed, light and other environmental factors may have an impact on the test results, this test will be completed indoors as shown in Fig. 7.

Fig. 7 - Test system for centrifugal nozzle parameters

1 - Centrifugal nozzle; 2 - Support frame; 3 - Guide rails; 4 - Laser particle size analyzer analysis software; 5 - Laser particle sizer

Test results analysis

As shown in Fig. 8, the droplet size is related to the supply flow rate and nozzle speed, and the higher the flow rate and the lower the speed, the larger the droplet size. At the same flow rate, the higher the rotational speed, the smaller the droplet size. Fig. 8b shows the nozzle test Dv50 data, in the nozzle speed from 8000 r/min to 12000 r/min process, the droplet size changes in a larger magnitude, the speed reaches 12000 r/min after the size change curve tends to flatten.

When the nozzle rotational speed is the same, the effect of the liquid supply flow rate on the droplet particle size is not consistent, the flow rate being in the interval of 500 mL/min to 650 mL/min, 800 mL/min to 1000 mL/min, the degree of change in the droplet particle size at different centrifugal rotational speeds is relatively small compared to the degree of change in the droplet particle size outside the flow rate interval. Centrifugal atomizing nozzles have small droplet size distribution and narrow droplet spectrum width, which have obvious advantages over pressure atomizing nozzles. Combined with Fig. 8a and 8c, it can be seen that in the parametric test of a single nozzle, by adjusting the liquid supply flow rate and nozzle rotation speed, a number of droplets can have a particle size of less than 35 μm. For example, if the liquid supply flow rate is 650 ml and the nozzle rotation speed is 14,000 r/min, the Dv10 data is 43.263 μm, the Dv90 data is 118.753 μm, and the Dv50 data is 74.357 μm, according to the fog droplet spectral width representation equation:

$$\frac{D_{V90}-D_{V10}}{D_{V50}} \tag{1}$$

The width of the droplet spectrum can be obtained as 1.02 less than 2.0, which is in line with the quality technical index of spraying operation.

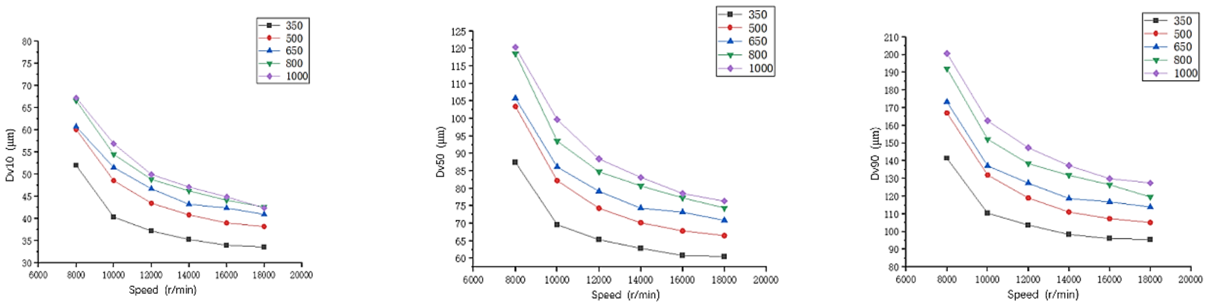

a) *b)* *c)*

Fig. 8 - Flow rate, rotational speed and particle size of droplets

There is a relationship between droplet size and pesticide efficacy of bio-optimal particle size, pesticide spraying technology theory research that the control of flying pests is suitable for the use of small insecticide droplets of 10 to 50 μm, the control of foliar crawling pest larvae is suitable for the use of insecticide droplets of 30 to 150 μm, the spraying of fungicide control of plant diseases is suitable for the use of droplets of 30 to 150 μm, and herbicide spraying is suitable for the use of coarse droplets of 100 to 300 μm (*Chen et al., 2021; Uk et al., 1997; Yuan et al, 2015; Zhang et al., 2022*). Considering the factors of droplet evaporation, drift, penetration, and droplet adhesion on leaves, the centrifugal nozzle parameters in this paper were selected to supply liquid at a flow rate of 1,000 mL/min, and the nozzle rotational speed was 14,000 r/min.

DROPLET DISTRIBUTION CHARACTERIZATION TEST AND RESULT ANALYSIS

Experimental site and conditions

The experiment was conducted on September 10, 2022 at the test site of Anhui Agricultural University, Anhui Province, China. The maize planted in the trial site was a late-maturing fresh maize variety, which was in the filling stage at that time, with an average plant height of about 200 cm, planting row spacing of 60 cm, and an average plant spacing of 25 cm. The day of the trial was a sunny day, with an average air temperature of 21°C, an easterly wind, a wind speed of 0.6-1.2 m/s, and a relative humidity of 48%. In order to reduce the effect of morning and evening field fog, the experiment was selected in the afternoon.

Experimental material

Fog droplet sampling uses water-sensitive test paper with a specification of 35 mm × 110 mm, with a yellow background color that changes to blue when exposed to water, which can be used to detect the distribution status of fog droplets in the field.

Experimental design

In the experimental field, a 30m×20m experimental area was selected for sampling point arrangement, three collection strips with 5 m interval were set up, six maize plants with 1 m interval were selected for each collection strip, and three layers of vertical sampling points were set up for each maize plant at a distance of 0.3 m from the ground (bottom), 1 m (middle), and 1.7 m (canopy), and water-sensitive test papers were arranged on the maize leaves at each sampling point to form a three-dimensional sampling point. Each sampling point was arranged with water-sensitive test paper on maize leaves to form a three-dimensional sampling point. The schematic layout of the field test paper is shown in Fig. 9. The UAV flight path was operated according to the arrow direction, and the sampling belt was located in the middle of the spray pattern extending to both sides. According to the results of the matching test calculations of the parameters of plant protection UAV flight height, operation width and application amount in the previous experiments and the related articles on the impact of plant protection UAV parameters on maize plant protection (*Wang et al., 2023; Qin et al., 2014*), the flight height of the UAV was set to 4 m, and water was used instead of pesticide for the test. During the test, the UAV used the conventional reciprocating flight application mode to carry out spraying operations on maize, and the interval between each route was 3 m. A schematic diagram of the test paper arrangement for the field test is shown in Fig. 9. The test plot was open and unobstructed, and the maize growth was more consistent.

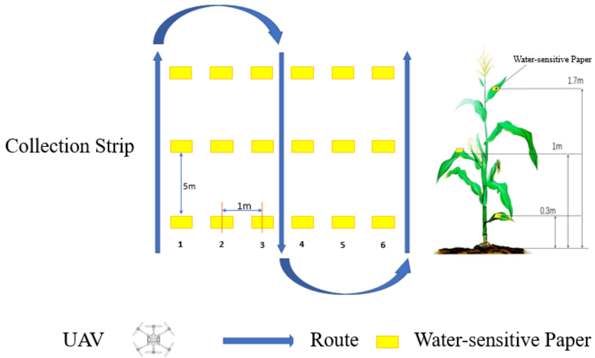

Fig. 9 - Schematic layout of water-sensitive test strips

Three common speed sorties (*Wang et al., 2021*), 1.5 m/s, 3 m/s and 4.5 m/s treatments, were set up for testing the droplet deposition distribution characteristics of UAV sprayed droplets at different sampling locations in maize plants under different flight speeds, and the specific experimental parameters are shown in Table 1.

Table 1

Test design for droplet distribution characteristics

Sortie	Speed (m/s)	Height (m)	Flux (L·min)	Nozzle Speed (r/min)
1	1.5m/s	4m	4	14000
2	3m/s	4m	4	14000
3	4.5m/s	4m	4	14000

Data collection and processing

After the completion of each set of tests the water sensitive papers were collected one by one in a sealed bag by serial number and brought back to the laboratory for processing. A scanner was used to scan the collected water-sensitive paper into a grayscale image with a resolution of 600 dpi and saved in jpg format. The scanned images were imported into the image processing software Deposit Scan and analyzed to obtain the deposition characteristics, including droplet density, coverage, deposition volume and other parameters.

In order to characterize the uniformity of droplet deposition among the collection points in the test, it can be evaluated by the coefficient of variation (CV) of the density of droplet coverage (or deposition) at different collection points within the effective spraying area of the UAV, and the smaller the value is, the better the droplet uniformity is. The coefficient of variation (CV) is calculated as:

$$CV=\frac{SD}{\overline{X}}\times 100\% \quad (2)$$

$$SD=\sqrt{\sum_{i=1}^{n}\frac{(X_i-\overline{X})^2}{N-1}} \quad (3)$$

where:

SD is the standard deviation of the same group of test collection samples; Xi is the droplet density (or deposition) of each collection point; $\overline{X}$ is the average value of droplet density (or deposition) of each group of test collection points; N is the number of test collection points of each group.

RESULTS AND ANALYSES

Particle size distribution of droplets at different flight speeds

Figure 10 shows the comparison of the droplet volume median diameter (VMD) at different sampling locations for each test sortie, from which it can be seen that at the same sampling level, the value of VMD decreases with the increase of the flight speed from 1.5 m/s to 4.5 m/s; the flight speed significantly affects the droplet size at the same sampling level. For example, in the bottom layer of maize plants, the corresponding droplet volume median diameters at flight speeds of 1.5, 3, and 4.5 m/s were 98.87, 75.67, and 72.73 μm, respectively.

The droplet volume median diameters at 3 m/s decreased by 35.94% compared with that at 1.5 m/s. The basic trend of VMD in different sampling layers at the same speed was maximum in the canopy layer, followed by the middle layer and minimum in the bottom layer. However, when the UAV flight speed was 1.5 m/s, it can be seen from the figure that the VMD of the bottom layer was 98.87 μm larger than that of the middle layer, 92.64 μm, which was opposite to the results of 3 m/s and 4 m/s.

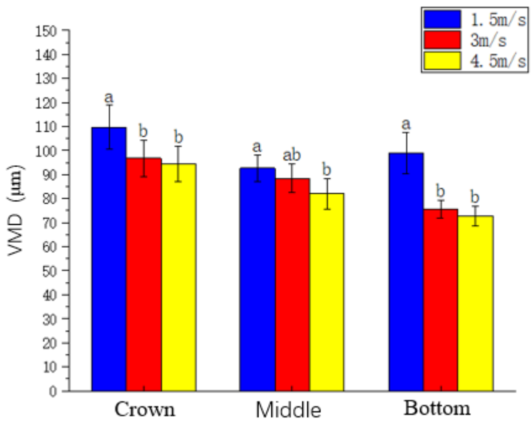

Fig. 10 - Particle size distribution of droplets at different flight speeds

(Data in the table are mean ± standard error. Different lowercase letters in the same column indicate that the different treatments were tested by Turkey's method at the P<0.05 level)

Characterization of droplet deposition at each sampling point at different flight speeds

There is a close relationship between droplet coverage density and droplet size, application rate and flight speed. Under the same droplet size and application rate, it can be seen in Fig.11 that among the three flight speeds of the experimental treatments, the droplet coverage density of each sampling point under the same speed has the same trend with the sampling position, and the droplet coverage density of the bottom layer is the largest at 1.5 m/s, the droplet coverage density of the canopy layer is the largest at 3 m/s and 4.5 m/s, and the maximum droplet coverage density of the three speeds occurs in different positions.

The maximum droplet coverage density at the slower speed of 1.5 m/s was 432.09 droplets/cm^2 at the bottom of sampling point 1, and the minimum was 41.43 droplets/cm^2 at the bottom of sampling point 6 at the speed of 4.5 m/s. This experiment used the same multi-route reciprocal spraying as the actual operation, and it can be seen that the droplet deposition pattern is highly consistent among the collection points in the spraying area of the UAV under the same treatment.

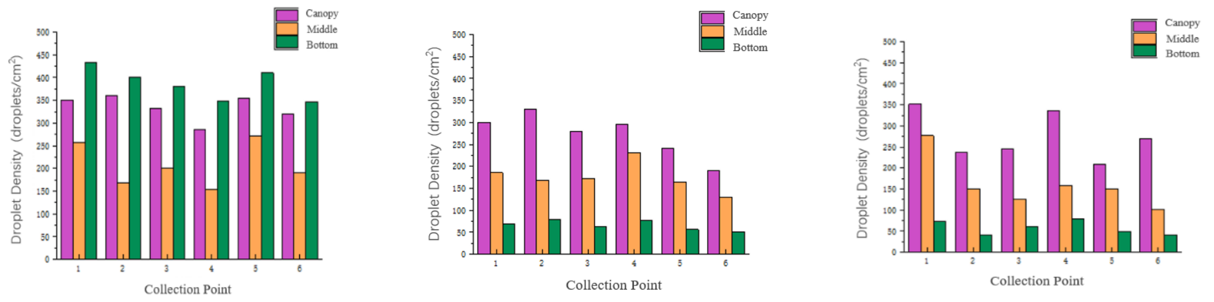

(a) 1.5 m/s (b) 3 m/s (c) 4.5 m/s

Fig. 11 - Distribution of droplet deposition characteristics at each sampling point for different flight speeds

Analysis of droplet density, coverage and droplet deposition

Table 2

Parameters of droplet deposition characteristics for each sampling layer

Sampling Point	Sortie	Droplet Density (droplets/cm^2)	Coefficient of Variation of Droplet Density	Deposition (μm/cm^2)	Coefficient of Variation of Deposition	Coverage (%)	Coefficient of Variation of Coverage
Canopy	1	334.16±28.14^a	8.42	0.313±0.02^a	5.55	23.63±1.9^a	7.86
	2	273.05±50.02^a	18.32	0.297±0.07^a	24.27	14.44±4.7^b	32.39
	3	274.48±57.52^a	20.96	0.287±0.09^a	31.33	13.15±6.3^b	48.19
Middle	1	206.44±47.27^a	22.90	0.171±0.05^a	29.80	8.19±2.6^a	31.91
	2	174.94±32.97^a	18.85	0.138±0.05^a	35.34	7.53±2.3^a	30.23
	3	160.19±60.91^a	38.02	0.118±0.07^a	58.67	4.95±2.9^a	58.44
Bottom	1	386.29±34.72^a	8.99	0.365±0.04^a	11.07	28.21±3.9^a	13.72
	2	65.52±11.45^b	17.48	0.040±0.01^b	27.25	3.09±1.1^b	34.09
	3	57.47±16.14^b	28.10	0.034±0.01^b	33.05	1.63±0.6^b	38.10

(Data in the table are mean ± standard error. Different lowercase letters in the same column indicate that the different treatments were tested by Turkey's method at the $P<0.05$ level)

Table 2 shows the droplet deposition parameters of each sampling level, and it is not difficult to find that the flight speed significantly affects the droplet coverage, droplet density and deposition amount of the same sampling level, and the trends of droplet coverage and droplet deposition amount of each sampling level (canopy, middle and bottom) decrease with the increase of the flight speed, and only the droplet density of the canopy level of sorties 2 and 3 (with the flight speed of 3 m/s and 4.5 m/s) do not conform to this law, but the values of the two were very close to each other. In the canopy sampling position, the average droplet density of sortie 1 (flight speed of 1.5 m/s) reached 334.16/cm^2, and the extreme difference between the sorties was 61.11/cm^2, but the difference was not significant ($P=0.064$). Similarly, the droplet densities in the middle layer were 160.19~206.44 droplets/cm^2, which was not significant, but the droplet densities in the bottom layer were significant, and the droplet density in the bottom layer of flight 1 exceeded the droplet density in the canopy layer to reach 386.29 droplets/cm^2, and the minimum droplet density in the bottom layer of flight 3 was 57.47 droplets/cm^2, which was much smaller than the droplet density in the canopy layer. The reason for this is that, when the flight speed is small, the downwash airflow reaches the ground and spreads upward to a certain height, which leads to the obvious difference in the bottom layer data. The pattern of change of droplet deposition and droplet density of each sortie is generally consistent, the maximum deposition is in the bottom layer of sortie 1, and the minimum value is in the bottom layer of sortie 3, which is 0.365 μm/cm2 and 0.034 μm/cm^2, respectively.

A comprehensive analysis of the data in Table 4 reveals that under the operational treatments in this study, the difference in the fog droplet deposition effect at flight speeds of 3 m/s and 4.5 m/s is not significant, but the difference between these two sorties and the fog droplet deposition effect at a flight speed of 1.5 m/s is more significant. In this study, the coefficient of variation CV value was used to measure the uniformity of fog droplet deposition among the collection points within the UAV spraying area in the experiment.

Table 4 shows that the coefficients of variation for droplet deposition, droplet coverage and droplet density at 1.5 m/s are smaller than those of the other two groups, which indicates that under the operating conditions of this paper, the droplet deposition effect of the centrifugal spraying system of the maize plant protection drone is most uniform at a flight speed of 1.5 m/s. The coefficients of variation for droplet density at the maize crown, middle and lower layers at both the flight speeds of 1.5 and 3 m/s are less than 50%, which is in line with the provisions of MH/T 1002.1-2016 "Quality Technical Indicators of Agricultural Aerial Operations Part 1: Spraying Operations" on the uniformity of droplet distribution in constant spraying operations, and the coefficient of variation of droplet density in the middle layer at a flight speed of 4.5 m/s was 58.44% slightly higher than the operational standard. Considering the requirements of actual operation on the efficiency of the UAV and the utilization rate of pesticides, a flight speed of 3 m/s can be considered for operation in actual operation.

CONCLUSIONS

In this paper, a set of maize plant protection UAV centrifugal spraying system was designed based on DJI T20 UAV platform, and the performance test of single nozzle and the field test of the droplet distribution characteristics of the whole system under different flight speeds were carried out. According to the analysis of the experimental results in this study, the coefficient of variation of fog droplet density in the crown, middle and lower layers of maize at 1.5 m/s and 3 m/s flight speeds is less than 50%, which is in line with the provisions of the quality technical indexes of agricultural aerial operations. When the flight speed is 4.5 m/s, the coefficient of variation of droplet density in its middle layer is 58.44% which is slightly higher than the operation standard, and the coefficients of variation of the crown and the bottom layer are also in accordance with the regulations. A flight speed of 3 m/s can be considered for the actual operation.

ACKNOWLEDGEMENT

This work was supported by Anhui Provincial Science and Technology Special Project, No.2022296906020008.

REFERENCES

[1] Biglia, A., Grella, M., Bloise, N., et al. (2022). UAV-spray application in vineyards: Flight modes and spray system adjustment effects on canopy deposit, coverage, and off-target losses. *The Science of the total environment*, Vol. 845, 157292.

[2] Chen, C., Li, S., Wu, X., et al. (2021). Analysis of droplet size uniformity and selection of spray parameters based on the biological optimum particle size theory. Environmental research, Vol. 204 (Pt B), 112076.

[3] Chen, J., Liu, W., Yuan, Y. (2018). Current status and development trend of the use of drone atomising nozzle (无人机雾化喷头的使用现状与发展趋势). *China Plant Protection Guide*, Vol. 38, Issue 03, 66-70.

[4] Chen, Q., Zhang, J., Zhang, C., et al. (2023). CFD analysis and RBFNN-based optimization of spraying system for a six-rotor unmanned aerial vehicle (UAV) sprayer. *Crop Protection*, Vol.174, Issue 106433, 0261-2194.

[5] Chen, S., Lan, Y., Bradley, K. F., et al. (2017). Effect of wind field below the rotor of a multi-rotor UAV on aerial spraying droplet deposition (多旋翼无人机旋翼下方风场对航空喷施雾滴沉积的影响). *Journal of Agricultural Machinery*, Vol. 48, Issue 08, 105-113.

[6] Dong, K., Chen, H., Zheng, Y., et al. (2018). Design and test of centrifugal nozzle for plant protection drone (植保无人机离心喷头的设计与试验). *Journal of China University of Metrology*, Vol. 29, Issue 03, 265-268.

[7] Fritz, B. K., Hoffmann, W. C., Bagley, W. E. (2009). Effects of spray mixtures on droplet size under aerial application conditions and implications on drift. *Applied Engineering in Agriculture*, Vol. 26, Issue 1, 21-29.

[8] Liu, L., Sun, K., Zhang, Q., et al. (2022). Maize plant protection UAV hot dance spraying system design and droplet distribution characteristics test (玉米植保无人机热雾喷施系统设计与雾滴分布特性试验). *Journal of Agricultural Machinery*, Vol. 53, Issue 12, 80-88.

[9] Pankaj, G., Shashidhar, K. (2023). Experimental analysis of spray droplet deposition behaviour for centrifugal assisted spinning disc sprayer. *Materials Today: Proceedings*. Vol. 92, Issue 1, 258-263.

[10] Qin, W., Xue, X., Zhou, L., et al. (2014). Effects of unmanned helicopter spraying parameters on the distribution of droplet deposition in maize canopy (无人直升机喷雾参数对玉米冠层雾滴沉积分布的影响). *Journal of Agricultural Engineering*, Vol. 30, Issue 05, 50-56.

[11] Qiu, B., Wang, L., Cai, D., et al. (2013). Effects of flight height and speed of unmanned helicopter on spray deposition distribution (无人直升机飞行高度与速度对喷雾沉积分布的影响). *Journal of Agricultural Engineering*, Vol. 29, Issue 24, 25-32.
[12] Ru, Y., Fang, S., Xue, J., et al. (2023). Experimental study of the influence factors of the droplet size of rotary nozzles during manned helicopter spraying operations. *Crop Protection*, Vol. 177, 106550.
[13] Uk, S. (1977). Tracing insecticide spray droplets by sizes on natural surfaces. The state of the art and its value. *Pesticide Science*, Vol. 8, Issue 5, 501-509.
[14] Wang, C., Herbst, A., Zeng, A., et al. (2021). Assessment of spray deposition, drift and mass balance from unmanned aerial vehicle sprayer using an artificial vineyard. *Science of The Total Environment*, Vol. 777, Issue 146181, 0048-9697.
[15] Wang, L., Xu, M., Hou, Q., et al. (2021). Numerical verification on influence of multi-feature parameters to the downwash airflow field and operation effect of a six-rotor agricultural UAV in flight. Computers and Electronics in Agriculture, Vol. 190, 106425.
[16] Wang, Z., Hussain, M., Yin, J., et al. (2023). Analysis of droplet deposition and maize (*Zea Mays l*.) growth control: application of ethephon by small unmanned aerial vehicle and electric knapsack sprayer. *Field Crops Research*. Vol. 292, 108822
[17] Xie, D., Chen, L., Liu, L., et al (2022). Actuators and sensors for application in agricultural robots: A review. Machines, Vol. 10, Issue 10, 913.
[18] Yang, Y., Zhang, B., Zha, J. et al. (2020). Real-time extraction of navigation lines between rows of maize (玉米行间导航线实时提取). *Journal of Agricultural Engineering*, Vol. 36, Issue 12, 162-171.
[19] Yuan, H., Wang, G. (2015). Relationship between droplet size and coverage density and pesticide control effect (雾滴大小和覆盖密度与农药防治效果的关系). *Plant Protection*, Vol. 41 Issue 06, 9-16.
[20] Zhang, H., Lan, Y., Wen, S., et al. (2022). Modelling the adhesion of fog droplets on rice plants under the action of UAV rotor wind field (无人机旋翼风场作用下雾滴在水稻植株上的黏附量模型构建). *Journal of Agricultural Engineering*, Vol. 38, Issue 18, 40-50.